**Journal of Electrotechnology, Electrical Engineering and Management (2026)**
**Clausius Scientific Press, Canada**
**DOI: 10.23977/jeeem.2026.090105**
**ISSN 2560-6697 Vol. 9 Num. 1**

# *Coordinated Voltage Regulation and Steady-State Operation Optimization for High-PV Distribution Networks*

**Xu Li***

*School of Electrical Engineering, Shen Guorong School, Nanjing Institute of Technology, Nanjing, Jiangsu, 211167, China*
**Corresponding author*

***Keywords:*** New power system, distribution network, voltage regulation, steady-state optimization, improved particle swarm optimization (IPSO)

***Abstract:*** With the rapid development of new power systems, the high penetration of distributed photovoltaic (PV) generation has created significant challenges for the steady-state operation of distribution networks. During periods of strong solar irradiation, the intermittency of PV output may lead to reverse power flow, voltage-limit violations, and increased network losses. To address these issues, this paper proposes a steady-state operation optimization and voltage-regulation strategy based on an Improved Particle Swarm Optimization (IPSO) algorithm. A single-snapshot optimization model is established to minimize active power loss and node-voltage deviation under a severe high-PV operating condition. The proposed IPSO incorporates a dynamic inertia-weight mechanism and a penalty-based treatment of discrete control variables, enabling coordinated optimization of PV-inverter reactive power and OLTC tap actions. Simulation results for a 33-bus radial distribution system show that the proposed strategy reduces active power loss by more than 70% compared with the unoptimized high-PV scenario, while maintaining all node voltages within the allowable range of 0.95–1.05 p.u. These results demonstrate the effectiveness of the proposed method for improving feeder operating performance under high-PV penetration conditions.

## 1. Introduction

With the continuous advancement of the global energy transition, the concept of new power systems has been widely promoted. A defining feature of this transition is the high penetration of distributed renewable energy, particularly photovoltaic (PV) generation, in distribution networks. Although this transformation contributes significantly to carbon-emission reduction, the intermittent and stochastic nature of PV output has introduced substantial challenges to the steady-state operation of regional distribution systems. Under high-irradiance conditions, reverse power flow may occur in radial feeders, which can further lead to node overvoltage, increased network loss, and deteriorated operating security .

To address these issues, steady-state operation optimization and effective voltage regulation are essential for active distribution networks. In general, the key objectives include minimizing active power loss and reducing node voltage deviation while maintaining operational economy and device safety . Traditional voltage regulation mainly depends on discrete mechanical devices such as On-Load Tap Changers (OLTCs) and switched capacitor banks. However, because these devices have limited switching frequency and relatively slow response speed, they are not well suited to track the rapid fluctuation of PV generation. Consequently, increasing attention has been paid to the coordinated control of discrete devices and fast continuous regulation resources, such as PV inverter reactive power support and distributed battery energy storage systems, in order to achieve more flexible voltage regulation. Meanwhile, data-driven methods such as deep learning have also been introduced into power control and loss reduction problems, but their deployment often depends on abundant training data and considerable computational resources, which may limit their practical application in conventional distribution-network operation. In a broader sense, the challenge is not only a local voltage-quality issue, but also part of the wider control-and-stability transformation caused by renewable-dominated power systems. This background makes it necessary to design voltage-regulation strategies that remain simple enough for feeder-level implementation while still responding effectively to rapid PV fluctuations[1].

From the viewpoint of mathematical optimization, coordinated voltage regulation involving OLTC tap positions and inverter reactive power outputs is a mixed discrete-continuous, nonlinear optimization problem with multiple constraints. Traditional mathematical programming methods may face difficulties in convergence robustness and computational efficiency when the search space becomes highly nonconvex. For this reason, heuristic intelligence algorithms, especially Particle Swarm Optimization (PSO), have been widely applied to reactive power optimization and voltage-profile improvement because of their simple structure, ease of implementation, and strong global search ability. To enhance the original PSO, a variety of Improved Particle Swarm Optimization (IPSO) strategies have been proposed for distribution-network applications. Nevertheless, many existing approaches still show limitations when discrete control variables and continuous control variables must be handled simultaneously, and they may suffer from premature convergence or insufficient constraint-handling capability[2].

Related studies have approached the voltage-regulation problem from different angles. Jafari et al. coordinated OLTC and PV inverters in a decentralized manner and showed that reactive power support from inverters can relieve excessive OLTC operations under high-PV conditions. Chen et al. further demonstrated that coordinated distributed BESS control can mitigate voltage fluctuations in low-voltage networks, especially when communication-assisted coordination is available. Under disturbed operating conditions, coordinated PV-inverter control has also been investigated for voltage support during fault events. In addition, loss-reduction and voltage-improvement studies based on network reconfiguration, DG sizing, and DG placement have confirmed that voltage quality and active-power loss are strongly coupled in distribution-network operation. These studies provide useful insights, but some of them focus on planning variables, some rely on additional storage or communication infrastructure, and others do not explicitly address the mixed discrete-continuous optimization structure created by OLTC taps and inverter reactive power in a compact operational framework[3].

In view of the above issues, this paper proposes an adaptive voltage regulation and steady-state operation optimization strategy for distribution networks based on IPSO. The main contributions are summarized as follows. First, a single-snapshot multi-objective optimization model is established by jointly considering active power loss and node voltage deviation under a severe high-PV operating condition. Second, an IPSO-based solution framework is designed by incorporating a dynamic inertia-weight strategy and a penalty mechanism for discrete control variables, so as to balance global exploration and local exploitation while improving constraint satisfaction. Third, the proposed strategy is illustrated on a 33-bus radial feeder framework to demonstrate its effectiveness in voltage-violation mitigation and loss reduction under a representative high-PV scenario. Compared with methods that require broader device coordination or communication-dependent architectures, the present framework aims to retain a relatively simple optimization structure while preserving practical control interpretability[4].

## 2. System Modeling and Problem Formulation

To evaluate the steady-state performance of the distribution network under high PV penetration, an optimization model is established for coordinated voltage regulation. The purpose of the model is to determine the optimal settings of control variables, including OLTC tap positions and PV inverter reactive power outputs, while satisfying the physical constraints of network operation. In this study, the model is formulated for feeder-level operational decision making rather than long-term planning. Accordingly, the optimization variables are selected from those control actions that can be adjusted directly during operation, whereas structural planning variables such as feeder reconfiguration or permanent DG relocation are not included. This modeling choice is consistent with the practical objective of mitigating a short-term overvoltage condition caused by concentrated PV generation while maintaining a manageable optimization dimension[5].

### 2.1 Objective Functions

In this study, a multi-objective optimization framework is adopted to improve the overall operating performance of the distribution network. Unlike multi-period scheduling, the present work focuses on a single-snapshot steady-state optimization under a severe operating condition. Therefore, the optimization objectives are restricted to the electrical-state performance of the network. This choice is intentional. For a high-PV noon snapshot, the most important operational concerns are whether the feeder voltages remain inside their allowable band and whether the corresponding power-flow pattern introduces unnecessary active-power loss. A compact two-objective formulation is therefore sufficient to capture the main trade-off between economy and voltage quality, and it also avoids introducing excessive modeling complexity that would be difficult to justify in a short engineering paper[6].

#### 2.1.1 Active Power Loss Minimization

The first objective is to minimize the total active power loss in the network branches. The corresponding objective function is written as

$$f_1=P_{\mathrm{loss}}=\sum_{k=1}^{N_L} R_k \frac{P_k^2+Q_k^2}{V_k^2} \tag{1}$$

where $N_L$ is the total number of branches, $R_k$ is the resistance of branch $k$, $P_k$ and $Q_k$ are the active and reactive power flows of branch $k$, respectively, and $V_k$ denotes the voltage magnitude associated with the receiving end of branch $k$.

#### 2.1.2 Voltage Deviation Minimization

To maintain acceptable voltage quality, the node voltages should remain as close as possible to the nominal value. The voltage-deviation objective is defined as

$$f_2=\sum_{j=1}^{N_B}\left|\frac{V_j-V_{\mathrm{ref}}}{V_{\mathrm{ref}}}\right| \tag{2}$$

where $N_B$ is the total number of buses, $V_j$ is the voltage magnitude of bus $j$, and $V_{\mathrm{ref}}$ is the reference voltage, which is typically taken as 1.0 p.u.

For solution by IPSO, the above objectives are combined into a weighted single-objective form:

$$\min F=\omega_1 f_1+\omega_2 f_2 \tag{3}$$

where $\omega_1$ and $\omega_2$ are nonnegative weighting coefficients satisfying

$$\omega_1+\omega_2=1 \tag{4}$$

## 2.2 System Constraints

The optimization problem is subject to both equality constraints and inequality constraints.

### 2.2.1 Equality Constraints

The equality constraints are the active and reactive power-balance equations at each bus:

$$P_{Gi}-P_{Di}-V_i\sum_{j=1}^{N_B}V_j\left(G_{ij}\cos\theta_{ij}+B_{ij}\sin\theta_{ij}\right)=0 \tag{5}$$

$$Q_{Gi}-Q_{Di}-V_i\sum_{j=1}^{N_B}V_j\left(G_{ij}\sin\theta_{ij}-B_{ij}\cos\theta_{ij}\right)=0 \tag{6}$$

where $P_{Gi}$ and $Q_{Gi}$ are the active and reactive power injections at bus $i$, $P_{Di}$ and $Q_{Di}$ are the active and reactive loads at bus $i$, $G_{ij}$ and $B_{ij}$ are the conductance and susceptance elements of the bus-admittance matrix, respectively, and $\theta_{ij}$ is the voltage angle difference between buses $i$ and $j$.

### 2.2.2 Inequality Constraints

The operational limits of the network and control devices can be described as follows.

The node-voltage limits are

$$V_{\min}\le V_i\le V_{\max} \tag{7}$$

where $V_{\min}$ and $V_{\max}$ are the lower and upper allowable voltage limits, respectively.

The OLTC tap-position limits are

$$\mathrm{Tap}_{\min}\le \mathrm{Tap}\le \mathrm{Tap}_{\max} \tag{8}$$

where the tap position is a discrete control variable.

The reactive power capability of each PV inverter is constrained by its apparent power rating and instantaneous active power output:

$$\left|Q_{\mathrm{PV},i}\right|\le\sqrt{S_{\mathrm{PV},i}^2-P_{\mathrm{PV},i}^2} \tag{9}$$

In practical applications, additional branch-current constraints and inverter power-factor constraints may also be included when required by the operating scenario.

## 3. Proposed Optimization Strategy

To solve the multi-objective mixed-integer nonlinear optimization problem formulated in Section 2, an Improved Particle Swarm Optimization (IPSO) strategy is adopted in this study. The conventional PSO algorithm is attractive because of its simple implementation and good global search capability[7]. However, direct application of standard PSO to distribution-network voltage regulation remains insufficient, since the decision variables include both continuous variables, such as PV inverter reactive power, and discrete variables, such as OLTC tap positions. In addition, the algorithm may suffer from premature convergence in a highly constrained nonconvex search space . Therefore, two targeted improvements are introduced. The motivation for retaining a PSO-type framework is twofold. First, the algorithm structure is easy to implement and modify for engineering optimization problems with mixed variable types. Second, compared with more elaborate data-driven or communication-intensive control schemes, a swarm-based search can be integrated with a conventional power-flow evaluation process in a relatively transparent manner. This makes the resulting optimization procedure easier to explain, reproduce, and tune for the illustrative 33-bus case considered in this paper.

### 3.1 Standard Particle Swarm Optimization

In the standard PSO algorithm, each particle represents a candidate solution in the search space. The particle position corresponds to a candidate coordinated control strategy, while the particle velocity reflects the search step in each decision dimension. In the present problem, these dimensions correspond to the inverter reactive-power settings and the OLTC tap variable. For the $i$th particle in the $d$th dimension at iteration $k$, the velocity and position are updated as

$$v_{id}^{k+1}=\omega v_{id}^{k}+c_1 r_1\left(pbest_{id}-x_{id}^{k}\right)+c_2 r_2\left(gbest_{d}-x_{id}^{k}\right) \tag{10}$$

$$x_{id}^{k+1}=x_{id}^{k}+v_{id}^{k+1} \tag{11}$$

where $\omega$ is the inertia weight, $c_1$ and $c_2$ are the cognitive and social acceleration coefficients, respectively, $r_1$ and $r_2$ are random numbers uniformly distributed in $[0,1]$, $pbest_{id}$ is the best position previously found by the particle, and $gbest_d$ is the best position found by the whole swarm.

### 3.2 Improved Particle Swarm Optimization

#### 3.2.1 Dynamic Inertia-Weight Strategy

The inertia weight has a direct impact on the balance between global exploration and local exploitation. If the inertia weight is fixed at a relatively large value, the particle swarm may keep exploring broadly but converge slowly. If it is fixed at a small value, the population may lose diversity too early and become trapped near a suboptimal region. To improve convergence performance, a linearly decreasing inertia weight is adopted:

$$\omega=\omega_{\max}-(\omega_{\max}-\omega_{\min})\frac{k}{K_{\max}} \tag{12}$$

where $\omega_{\max}$ and $\omega_{\min}$ are the initial and final inertia weights, respectively, $k$ is the current iteration number, and $K_{\max}$ is the maximum number of iterations. In the early search stage, a relatively large inertia weight helps the swarm explore the solution space more broadly, whereas in the later stage, a smaller inertia weight improves local refinement and convergence accuracy.

### 3.2.2 Discrete-Variable Handling and Penalty Design

Because the OLTC tap position is a discrete control variable, it cannot be directly optimized as a purely continuous quantity without additional treatment. This is one of the main differences between the present problem and many conventional continuous reactive-power optimization formulations. In the proposed strategy, the particle component corresponding to the tap position is first updated in continuous form and then mapped to the nearest admissible discrete tap. Meanwhile, a penalty term is introduced to discourage infeasible or nonphysical control states. In essence, this treatment allows the swarm to preserve the search flexibility of continuous updates while still guiding the particles back toward implementable control actions. The penalized fitness function is written as

$$F_{\text{pen}}=F+\lambda_1\sum\left|x_{\text{tap}}-\text{round}\left(x_{\text{tap}}\right)\right|+\lambda_2 C_{\text{viol}} \tag{13}$$

where $F$ is the weighted objective function defined in Section 2, $\lambda_1$ and $\lambda_2$ are penalty coefficients, $x_{\text{tap}}$ denotes the particle position associated with the tap variable, and $C_{\text{viol}}$ represents the aggregated constraint-violation term, such as voltage-limit or reactive-power-limit violations. Compared with using a rounding operation alone, this treatment improves the ability of the algorithm to search around feasible discrete solutions while maintaining convergence robustness.

## 3.3 Execution Procedure of the Proposed Strategy

The execution process of the IPSO-based coordinated voltage regulation strategy is summarized as follows:

1) Initialize the network data, load level, PV output scenario, and IPSO parameters, including swarm size, maximum iteration number, acceleration coefficients, and inertia-weight bounds.

2) Encode each particle as a coordinated control vector containing the reactive power outputs of the PV inverters and the OLTC tap variable.

3) Generate the initial particle positions and velocities within the allowable ranges of PV reactive power and OLTC tap positions.

4) Map the OLTC-related particle component to the nearest admissible discrete tap so that the candidate solution can be evaluated in a physically meaningful manner.

5) Perform power-flow calculation for each particle, evaluate the objective functions, and compute the penalized fitness value.

6) Check voltage and reactive-power-limit violations, and incorporate the corresponding violation severity into the penalty term.

7) Update the personal best position of each particle and the global best position of the swarm according to the current fitness values.

8) Update particle velocities and positions according to the IPSO rules, including the dynamic inertia-weight adjustment.

9) Repeat the evaluation and update cycle until the stopping criterion is satisfied or the maximum iteration number is reached.

10) Output the optimal coordinated control strategy and use it to analyze the resulting voltage profile, network loss, and convergence behavior.

The above procedure emphasizes the practical interpretation of the IPSO search. At each iteration, the candidate control vector is not evaluated abstractly, but through a power-flow-based operational check of the feeder. This makes the optimization results easier to interpret from an engineering point of view, since every fitness update is directly associated with voltage performance, active-power loss, and feasibility of the control action.

## 4. Simulation and Results

To verify the feasibility of the proposed coordinated voltage-regulation strategy, illustrative simulations are conducted.

### 4.1 Simulation Setup

An illustrative 33-bus radial system based on the IEEE 33-bus framework is adopted, with a base voltage of 12.66 kV and a total active power load of 3.715 MW. To simulate a representative high-penetration PV scenario, large-scale PV capacities are assumed to be integrated at the end nodes of the main feeder and its laterals (buses 18, 23, and 33). The detailed parameter settings of the integrated PV systems, including their active power generation and inverter capacity limits under the noon snapshot, are summarized in Table 1. The single-line diagram of the studied system is shown in Fig. 1.

Table 1: Detailed parameters and optimized reactive power outputs of the integrated PV systems.

| PV Plant | Node Location | Active Power $P_{PV}$ (kW) | Inverter Capacity $S_{PV}$ (kVA) | Optimized $Q_{PV}$ in Case 3 (kVar) |
|---|---|---|---|---|
| PV 1 | Bus 33 | 800 | 900 | -356.2 |
| PV 2 | Bus 18 | 750 | 850 | -328.4 |
| PV 3 | Bus 23 | 650 | 750 | -243.7 |

The analysis focuses on a single-snapshot steady-state optimization under a severe operating condition (e.g., peak solar irradiance at noon). This specific condition is prone to reverse power flows and overvoltage. The OLTC at the main substation is configured with 16 tap positions (±8 steps). The weighting coefficients for the comprehensive objective function are set to balance power loss reduction and voltage profile improvement ($\omega_1$=0.6 and $\omega_2$=0.4). This setting reflects the operational preference that voltage-security requirements should be satisfied without ignoring feeder economy. It also provides a simple way to compare the unoptimized and optimized cases without introducing a more complicated multi-scenario decision process.

Three illustrative scenarios are compared:

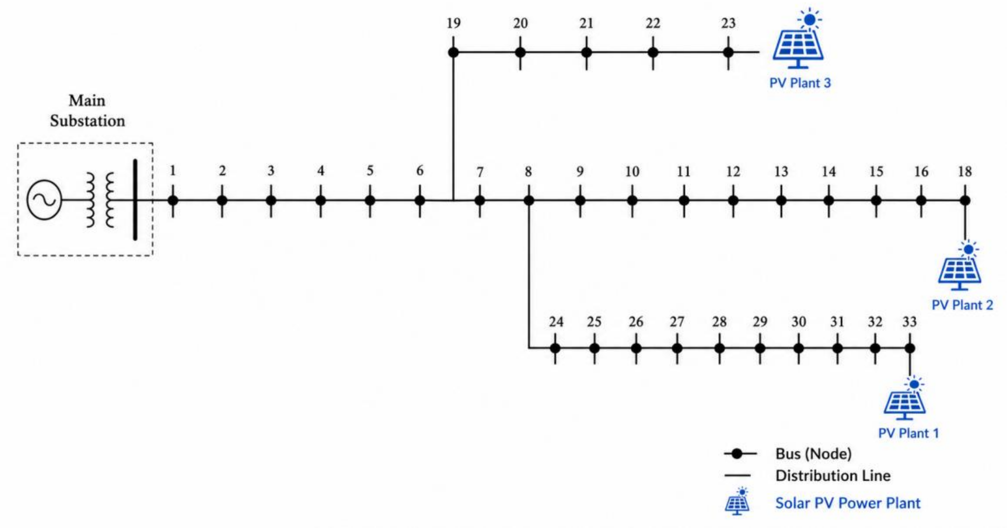


Figure 1: Illustrative single-line diagram of the studied 33-bus radial distribution system with PV integration.

- **Case 1 (Baseline):** The original network without PV integration.

- **Case 2 (Unoptimized High PV):** High PV penetration with PV inverters operating at unity power factor (no reactive power support) and the OLTC tap fixed at the nominal position.
- **Case 3 (Proposed IPSO):** High PV penetration coordinated by the proposed IPSO strategy.

### 4.2 Voltage Profile Analysis

Under the high-PV period in Case 2, the active power generated significantly exceeds the local load demand. The resulting reverse power flow pushes the voltages at the ends of the feeders upward. The simulation results show that the downstream node voltages exceed the upper safety limit of 1.05 p.u. and approach approximately 1.09 p.u., indicating a clear overvoltage risk under the selected operating condition[8].

When the proposed IPSO strategy (Case 3) is applied, the algorithm identifies a coordinated control combination. As detailed in Table 1, the PV inverters utilize their remaining inverter capacity to actively absorb a calculated amount of reactive power (e.g., -356.2 kVar at bus 33) to suppress the local voltage rise, where the negative sign indicates reactive power absorption rather than injection, while the OLTC steps down the substation voltage appropriately. The voltage profiles for all cases are compared in Fig. 2. In the optimized case, all bus voltages remain within the permissible operating range, indicating that the proposed coordination mitigates the severe overvoltage trend without relying on active power curtailment.

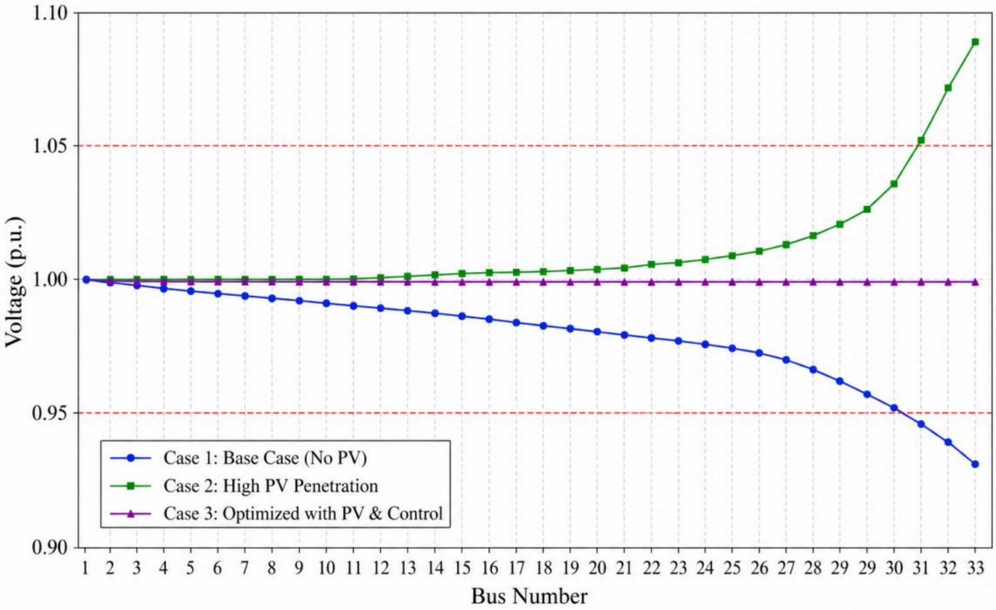


Figure 2: Voltage profile comparison of the 33-bus system under different scenarios.

### 4.3 Power Loss and Convergence Performance

Although PV integration in Case 2 may reduce part of the active power supplied by the main substation compared with the baseline case, the unoptimized high-PV operating condition still does not yield the minimum network loss. By dynamically optimizing the reactive power distribution, the proposed IPSO strategy in Case 3 further smooths the power flow. The total active power loss comparison is shown in Fig. 3. The simulation results show that the total active power loss decreases from approximately 96.4 kW in the unoptimized high-PV scenario to about 28.0 kW after optimization, corresponding to a reduction of more than 70%[9].

To further highlight the optimization effectiveness, Table 2 compares the standard PSO and the proposed IPSO in terms of total active power loss, maximum node-voltage deviation, and convergence iteration count. The results indicate that IPSO achieves a lower network loss and a smaller voltage deviation, while also converging in fewer iterations. This comparison is meaningful because both algorithms operate on the same optimization model and under the same operating assumptions. Therefore, the performance gap can be interpreted mainly as the effect of the proposed improvements in the search mechanism rather than a change in modeling conditions[10].

Table 2: Comparison of optimization performance between standard PSO and proposed IPSO

| Method | Total loss (kW) | Max. voltage deviation | Convergence iterations |
|---|---|---|---|
| Standard PSO | 31.6 | 0.044 | 38 |
| Proposed IPSO | 28.0 | 0.031 | 24 |

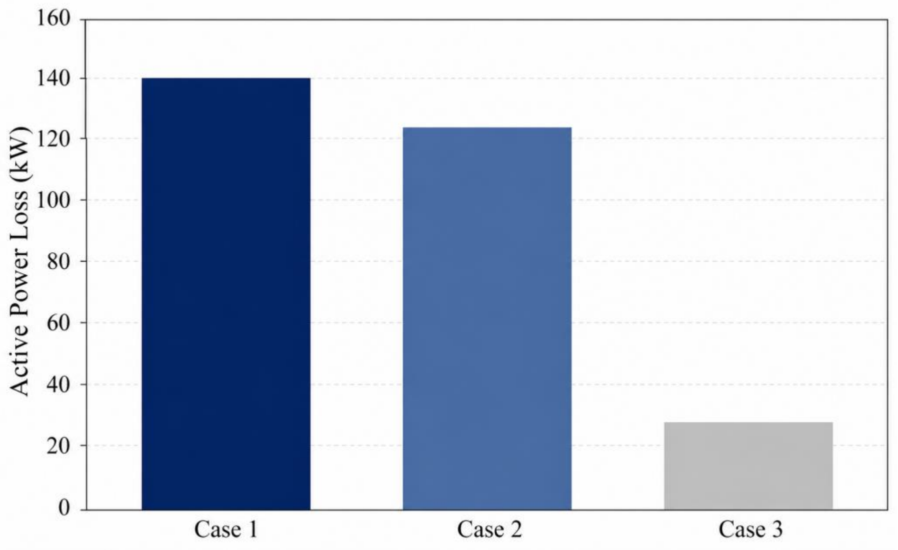


Figure 3: Comparison of total active power loss across different scenarios.

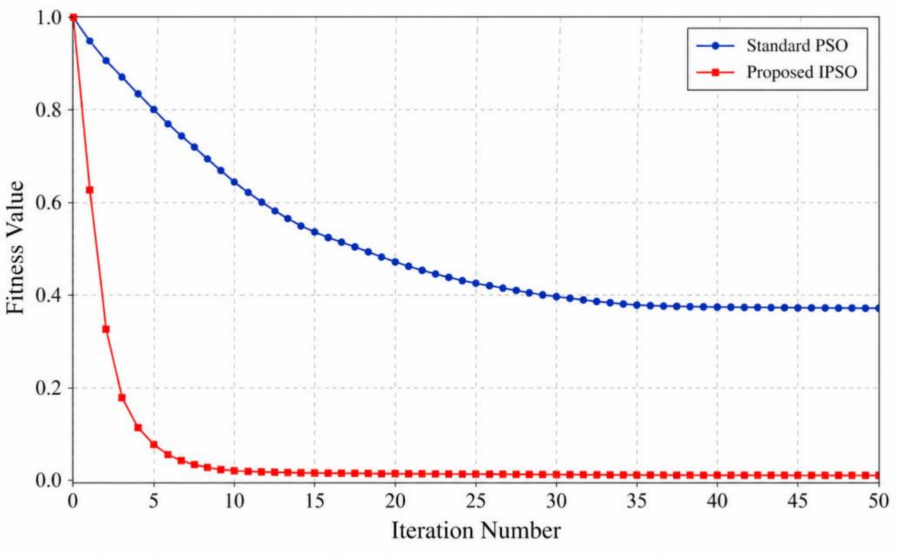


Figure 4: Algorithm convergence curve comparison between standard PSO and proposed IPSO.

Furthermore, the integration of the dynamic inertia weight and the discrete-variable penalty function enables the IPSO to navigate the mixed-integer search space efficiently. The convergence performance of the proposed algorithm is illustrated in Fig. 4. Compared with the standard PSO, the proposed IPSO reaches a stable solution more quickly in the early iterations and exhibits a smoother convergence trajectory, which supports its computational suitability for this optimization task. From an engineering perspective, this behavior suggests that the improved search process can identify a satisfactory coordinated control action with fewer ineffective oscillations among candidate solutions. In other words, the proposed IPSO does not merely produce a better final operating point; it also makes the optimization path more stable for the studied feeder-level problem.

## 5. Conclusion

This paper investigates a steady-state operation optimization and voltage regulation strategy for radial distribution networks with high PV penetration. Focusing on a severe noon operating snapshot, the study shows that large-scale PV integration may lead to reverse power flows and increase the risk of overvoltage. To address these issues, a coordinated voltage regulation strategy based on an Improved Particle Swarm Optimization (IPSO) algorithm is developed.

The formulated optimization model coordinates the discrete tap position of the OLTC with the continuous reactive power support from PV inverters. By incorporating a dynamic inertia weight and a discrete variable penalty function, the proposed IPSO algorithm demonstrates stable and fast convergence behavior in the studied case. The analysis of the 33-bus system indicates that the proposed strategy can bring node voltages back to the acceptable operating range and substantially reduce the active power loss level under the selected high-PV scenario. The comparative results with standard PSO further show that the proposed improvements are helpful not only for solution quality but also for convergence efficiency. Overall, the proposed method provides a practical and computationally efficient approach for steady-state voltage regulation in active distribution networks. Future work will extend the proposed strategy to multi-period dynamic voltage regulation and multi-scenario robust optimization for active distribution networks. It would also be meaningful to consider coordinated control with storage devices, communication constraints, and uncertainty in PV forecasting so that the method can be evaluated under more realistic active-distribution-network operating conditions.

## References

*[1] Q.-H. Wu, A. Bose, C. Singh, J. H. Chow, G. Mu, Y. Sun, Z. Liu, Z. Li, Y. Liu, Control and stability of large-scale power system with highly distributed renewable energy generation: Viewpoints from six aspects, CSEE Journal of Power and Energy Systems 9 (1) (2023) 8–14.*

*[2] S. You, Z. Jiang, H. Li, M. Bennett, X. Zhang, Y. Su, A. Till, J. Till, Y. Liu, Y. Liu, Impact of high pv penetration on regional power grids, in: 2022 7th IEEE Workshop on the Electronic Grid (eGRID), IEEE, 2022, pp. 1–5.*

*[3] M. Ntombela, K. Musasa, M. C. Leoaneka, Power loss minimization and voltage profile improvement by system reconfiguration, dg sizing, and placement, Computation 10 (10) (2022) 180.*

*[4] A. Chanane, M. Belazzoug, A new optimization approach to solve the optimal reactive power dispatch problem for real power loss minimization, voltage deviation minimization and voltage stability enhancement, in: 2024 3rd International Conference on Advanced Electrical Engineering (ICAEE), IEEE, 2024, pp. 1–5.*

*[5] M. R. Jafari, M. Parniani, M. H. Ravanji, Decentralized control of oltc and pv inverters for voltage regulation in radial distribution networks with high pv penetration, IEEE Transactions on Power Delivery 37 (6) (2022) 4827–4837.*

*[6] Z. Chen, E. I. Rogozinnikov, S. Geng, T. Liao, Coordinated control of distributed bess based on mas for voltage regulation in lv distribution network with high pv penetration, in: 2023 3rd Power System and Green Energy Conference (PSGEC), IEEE, 2023, pp. 234–238.*

*[7] S.-K. Chen, Y.-J. Liu, Y.-T. Yang, T.-C. Huang, C.-S. Chen, Coordinated control of distributed pv inverters for voltage regulation in the high-pv penetration distribution network under fault events, in: 2025 Seventh International Symposium on Computer, Consumer and Control (IS3C), IEEE, 2025, pp. 1–4.*

*[8] P. A. Babu, J. L. M. Iqbal, S. S. Priyanka, M. J. Reddy, G. S. Kumar, R. Ayyasamy, Power control and optimization for power loss reduction using deep learning in microgrid systems, Electric Power Components and Systems 52 (2)*

*(2024) 219–232.*
*[9] S. Bhuyan, M. Das, K. c. Bhuyan, Particle swarm optimizations based dg allocation in local pv distribution networks for voltage profile improvement, in: 2016 International Conference on Signal Processing, Communication, Power and Embedded System (SCOPES), IEEE, 2016, pp. 1–4.*
*[10] S. Gao, H. Wang, C. Wang, S. Gu, H. Xu, H. Ma, Reactive power optimization of low voltage distribution network based on improved particle swarm optimization, in: 2017 IEEE Conference on Energy Internet and Energy System Integration (EI2), IEEE, 2017, pp. 1–5.*